

Exclusive breakup of ${}^7\text{Li}$ incident on a proton target at 5.44 A MeV

A. Pakou,^{1,*} O. Sgouros,¹ V. Soukeras,¹ F. Cappuzzello,^{2,3} N. Keeley,⁴ L. Acosta,^{5,6} C. Agodi,² X. Aslanoglou,¹ S. Calabrese,^{2,3} D. Carbone,² M. Cavallaro,² A. Foti,^{3,6} G. Marquinez-Durán,⁷ I. Martel,⁷ M. Mazzocco,^{8,9} C. Parascandolo,¹⁰ D. Pierroutsakou,¹⁰ K. Rusek,¹¹ E. Strano,^{8,9} V. A. B. Zagatto,¹² and K. Zerva¹

¹*Department of Physics and HINP, The University of Ioannina, 45110 Ioannina, Greece*

²*INFN Laboratori Nazionali del Sud, via S. Sofia 62, 95125 Catania, Italy*

³*Dipartimento di Fisica e Astronomia, Università di Catania, via S. Sofia 64, 95125 Catania, Italy*

⁴*National Centre for Nuclear Research, ul. Andrzejaja Soltana 7, 05-400 Otwock, Poland*

⁵*Instituto de Física, Universidad Nacional Autónoma de México, México D.F. 01000, México*

⁶*INFN - Sezione di Catania, via S. Sofia 64, 95125 Catania, Italy*

⁷*Departamento de Ciencias Integradas, Facultad de Ciencias Experimentales, Campus de El Carmen, Universidad de Huelva, 21071 Huelva, Spain*

⁸*Departimento di Fisica e Astronomia, Università di Padova, via Marzolo 8, I-35131 Padova, Italy*

⁹*INFN - Sezione di Padova, via Marzolo 8, I-35131 Padova, Italy*

¹⁰*INFN - Sezione di Napoli, via Cinthia, I-80126 Napoli, Italy*

¹¹*Heavy Ion Laboratory, University of Warsaw, ul. Pasteura 5a, 02-093, Warsaw, Poland*

¹²*Instituto de Física da Universidade Federal Fluminense, Avenida Gal. Milton Tavares de Souza, Niterói, Brazil*

(Received 16 March 2017; published 24 April 2017)

An exclusive measurement of the breakup of ${}^7\text{Li}$ incident on a proton target was performed at 38.1 MeV (5.44 MeV/nucleon), probing the direct part of the excitation to the continuum. The two cluster constituents of ${}^7\text{Li}$, ${}^4\text{He}$, and ${}^3\text{H}$, were recorded in coincidence in the MAGNEX spectrometer and a silicon detector respectively. Both detection systems were set at forward angles and the measurement of both kinematical solutions allowed the determination of a breakup angular distribution over a wide angular range in the center-of-mass frame. Comprehensive simulations provided the detection efficiency of the system and via the appropriate kinematics the transformation of the cross sections from the laboratory to the center-of-mass reference frame. The experimental results are analyzed and discussed together with previous elastic scattering data using the Continuum Discretized Coupled Channels (CDCC) framework and are found to be in satisfactory agreement. It was found that while the breakup cross section was dominated by the nonresonant component, the most important influence on the elastic scattering was due to coupling to the $7/2^-$ resonance of ${}^7\text{Li}$.

DOI: [10.1103/PhysRevC.95.044615](https://doi.org/10.1103/PhysRevC.95.044615)

I. INTRODUCTION

With the advent of radioactive beam facilities, elastic scattering of exotic nuclei has proved to be a powerful tool for investigating channel coupling effects, especially at near barrier energies [1–3]. At the same time, research has continued into reactions induced by stable weakly bound nuclei [4]. Weakly bound nuclei present strong cluster structures with small separation energies and thus break up very easily. Breakup cross sections have been measured with the aim of extracting structure properties, for providing information relevant to astrophysics, and for exploring the influence of breakup coupling on the elastic scattering by enabling the strength of these couplings to be fixed accurately. Standard methods, for example the Continuum Discretized Coupled Channels (CDCC) approach, have been developed to study breakup and its influence on elastic scattering at near barrier energies. In many of these investigations strong coupling effects on the elastic scattering do not seem to be connected directly to the observation of large breakup or transfer reaction cross sections. Specifically, in Ref. [5] the authors investigated

breakup coupling effects on near barrier ${}^6\text{Li}$, ${}^7\text{Be}$, and ${}^8\text{B} + {}^{58}\text{Ni}$ elastic scattering in the CDCC approach. They observed the following paradox: ${}^6\text{Li}$, with a relatively small breakup cross section, exhibits an important breakup coupling effect on the elastic scattering, whereas ${}^8\text{B}$, with a large breakup cross section, shows a very modest coupling effect. Further investigation of this subject is necessary and will be pursued in this work.

Motivated by the above aspects, we present exclusive breakup measurements for ${}^7\text{Li}$ incident on a proton target which, together with the chosen energy, should ensure that the breakup cross section is dominated by direct (i.e. nonresonant) decay to the continuum. The ${}^7\text{Li}$ nucleus has a well established $\alpha + t$ cluster structure with a relatively large separation energy of 2.47 MeV in comparison with the $\alpha + {}^3\text{He}$ separation energy of 1.59 MeV of its radioactive mirror nucleus ${}^7\text{Be}$. The breakup fragments, α and t , may originate either from sequential and/or direct processes. By sequential breakup we mean excitation of a relatively long-lived resonant state in the ${}^7\text{Li}$ continuum which subsequently decays into an α particle and a triton, as opposed to direct breakup which omits the intermediate step of the excitation of the resonant state. As the available energy of the reaction in this experiment is 2.28 MeV, we excite only marginally the first resonant

*Corresponding author: apakou@cc.uoi.gr

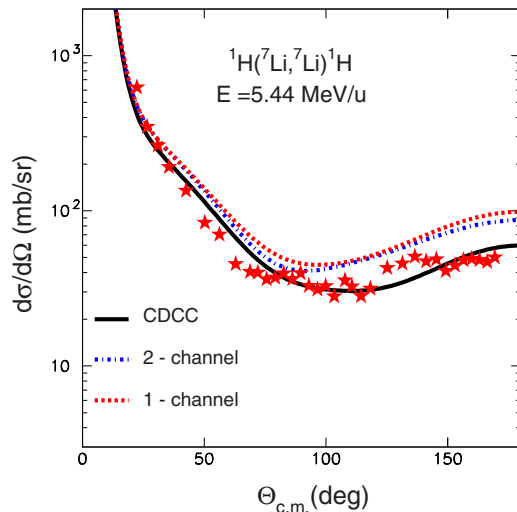


FIG. 1. Elastic scattering of ${}^7\text{Li} + p$ at 38.1 MeV. Details of the data collection and reduction are given in Ref. [6]. The solid black curve (labeled “CDCC”) denotes the full calculation, including couplings to the $\alpha + t$ continuum. The dotted red curve (labeled “1 - channel”) denotes the result of a calculation including ground state reorientation of ${}^7\text{Li}$ only. The dot-dashed blue curve (labeled “2 - channel”) denotes the result of a calculation including ground state reorientation and excitation of the 0.478 MeV $1/2^-$ bound first excited state of ${}^7\text{Li}$.

state of ${}^7\text{Li}$ at 4.63 MeV (2.16 MeV above the breakup threshold) and thus expect a very low contribution from resonant breakup to the total breakup cross section. Our analysis also includes the previously reported elastic scattering data [6], and both observables are interpreted simultaneously in the CDCC approach. The experiment was performed in inverse kinematics not only to mimic the situation with a radioactive beam, but also because the breakup fragments are thereby restricted to a small forward angular range in the laboratory system, increasing the statistical accuracy of the measurement but still preserving high angular resolution thanks to the use of the MAGNEX spectrometer [7]. The separation of the two kinematical solutions also allowed the determination of an angular distribution over a wide angular range in the center-of-mass frame.

The experimental setup has been described in detail elsewhere [6,8] and we will refer to it briefly in Sec. II. In the same section we will give information for the data reduction. Finally in Sec. III we will describe our CDCC approach for both elastic scattering and breakup on the same footing, with an appropriate discussion. This section will be followed by a summary.

II. EXPERIMENTAL DETAILS AND DATA REDUCTION

The experiment was performed at the Istituto Nazionale di Fisica Nucleare Laboratori Nazionali del Sud (INFN-LNS) in Catania, Italy. The ${}^7\text{Li}^{3+}$ beam was accelerated by the TANDEM Van de Graaff accelerator to 38.1 MeV and impinged on a $240 \mu\text{g}/\text{cm}^2$ CH_2 target, initially for an elastic scattering measurement. These results were reported in Ref. [6] but we present the angular distribution again in Fig. 1, together

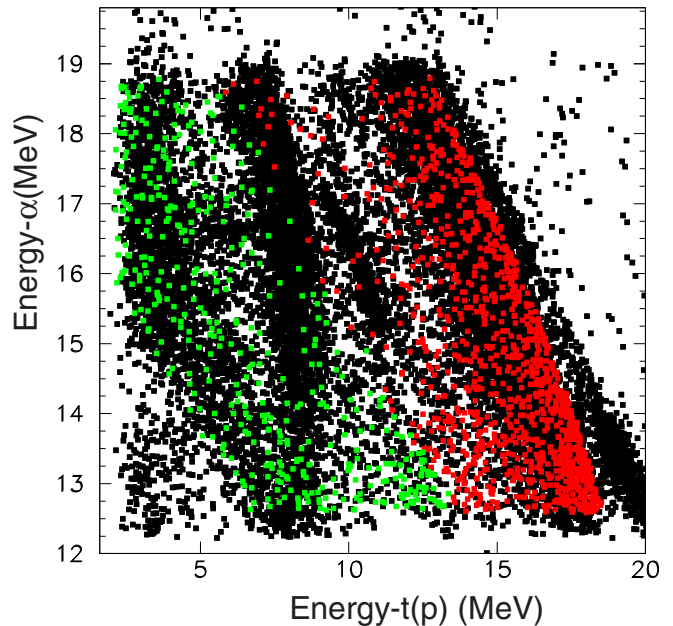


FIG. 2. Two dimensional energy spectrum determined at 38.1 MeV (5.44 MeV/nucleon) representing coincidence events of the two ${}^7\text{Li}$ breakup fragments: α energy versus triton or proton energy. The α 's were recorded in the MAGNEX spectrometer over an angular range of $\theta_{\text{lab}} = 0^\circ$ to 10° , while the tritons and recoiling protons were registered in a silicon detector set at $\theta_{\text{lab}} = 5^\circ$. Superimposed on the experimental spectrum, denoted in black, are simulations of the first and second kinematical solutions, denoted as red and green dots respectively. The simulation represents in an excellent way the data in the left- and right-hand loci originating from α 's in coincidence with tritons. The locus in the middle of the experimental (black) spectrum comes from coincidences of α 's with the recoiling protons.

with the results of CDCC calculations, described below. For the present exclusive breakup measurement a thicker target of $400 \mu\text{g}/\text{cm}^2$ was used to increase the statistics. The α fragments were momentum analyzed by MAGNEX [7] with the optical axis set at $\theta_{\text{opt}} = 4^\circ$ and detected by the focal plane detector [9,10]. The spectrometer worked with full horizontal angular acceptance and wide open vertical acceptance as the counting rate for this measurement was low, not affecting the silicon detectors of the focal plane. The elastically scattered ${}^7\text{Li}$ ions were “masked” by appropriate magnetic fields, allowing the detection of α 's in an energy slice between 12 and 19 MeV. A small remainder of elastic scattering was rejected offline by the appropriate cuts in two-dimensional ΔE vs $(\Delta E + E)$ spectra, obtained from the focal plane gas and silicon detectors [9]. The other breakup fragments, the tritons, were detected in a silicon detector set at $\theta_{\text{lab}} = 5^\circ$. This detector was masked by a $69.5 \mu\text{m}$ thick tantalum foil to prevent deterioration from Rutherford scattering. This foil absorbed all the α 's but allowed protons and tritons to pass. Protons were well discriminated from tritons as can be seen in Figs. 2 and 3. Figure 2 displays α -triton coincidence events and the two loci to the right and left of the figure, originating from the first and second kinematical solutions of the ${}^7\text{Li}$ breakup respectively, are well discriminated from recoiling protons in coincidence

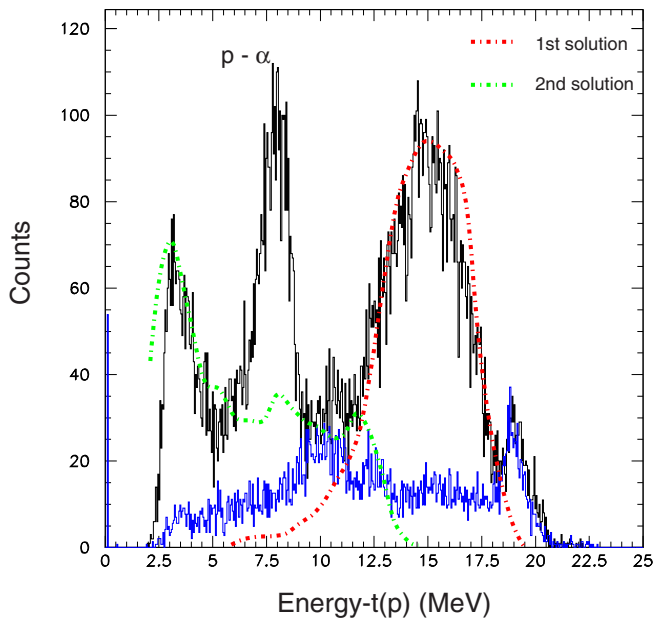


FIG. 3. Exclusive breakup spectrum acquired in the 5° silicon detector with the CH_2 target ($\alpha + t$ or p coincidences). Simulations for the first and second solution for $\alpha + t$ coincidences are denoted by the dot-dashed red and green lines respectively. The middle peak corresponds to $\alpha + p$ coincidences. The spectrum in blue represents an exclusive spectrum acquired with the carbon target, appropriately normalized.

with α 's (middle locus). Other observed loci are due to the carbon contained in the CH_2 target. These spurious loci can be identified in Fig. 4 which displays α -triton coincidences from the run with the carbon target. Note that the carbon background was $\sim 27\%$ and mainly affected the first solution. The one-dimension coincident spectrum acquired in the 5° silicon detector is displayed in Fig. 3 in black. Superimposed

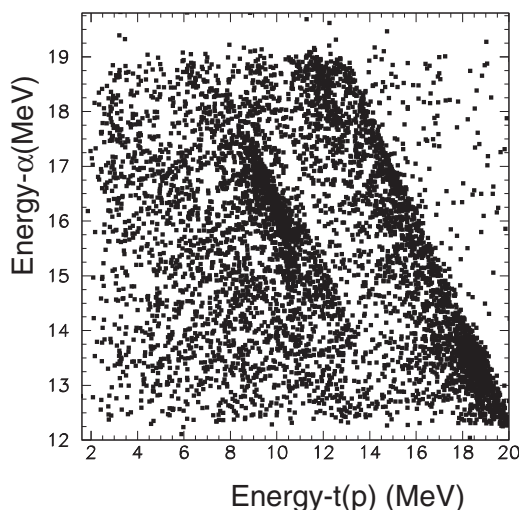


FIG. 4. As in Fig. 2 but for $\alpha + t$ coincidences from ${}^7\text{Li} + {}^{12}\text{C}$ breakup.

on the same figure in blue is a spectrum obtained with the carbon target, appropriately normalized.

The data reduction technique, based on the ray reconstruction of the data, is described in Refs. [11–14]. Exclusive yields were determined for pairs of angles every 0.5° for α 's observed in MAGNEX over the angular range 0° to 10° , combined with tritons observed at the fixed angle of 5° . This was done first for data acquired with the CH_2 target and then with the carbon one. Net yields were obtained by subtraction of the carbon yield appropriately normalized to flux and scattering centers of the CH_2 runs. The net yields were transformed to laboratory double differential cross sections ($d^2\sigma/d\Omega_\alpha d\Omega_t$) using a detection efficiency estimated with a Monte Carlo three-body simulation code [15] which took into account the ${}^7\text{Li} + p$ reaction leading to an excited state of ${}^7\text{Li}$ with an angular distribution obtained from a CDCC calculation, described below. The ${}^7\text{Li}$ randomly acquires an energy within one of the continuum bins specified in the CDCC calculation, either the resonant one at 4.63 MeV (2.163 ± 0.109 MeV above the breakup threshold) or one of the nonresonant ones. The excited lithium breaks into two fragments, α and triton, with one emitted with randomly specified energy and momentum and the other with energy and momentum fulfilling the usual conservation laws in the rest frame of the ${}^7\text{Li}^*$. The energy distributions of the fragments thus obtained are transformed to the laboratory system by imposing a Galilean transformation followed by the appropriate rotation. The simulated energy distributions for both kinematical solutions are presented in a two-dimensional α -vs-triton energy spectrum in Fig. 2 and a one-dimensional triton spectrum in Fig. 3. The excellent agreement between experiment and the simulation based on the

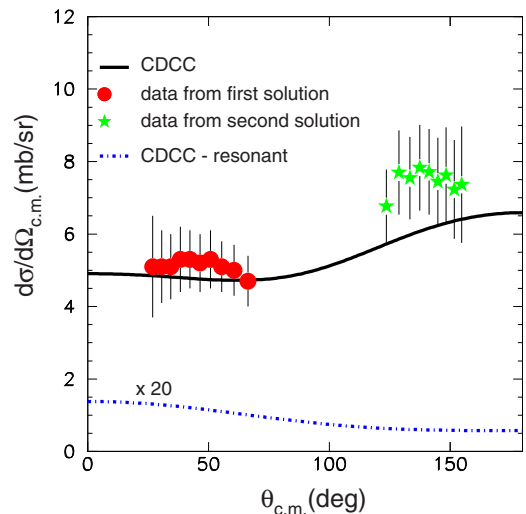


FIG. 5. Experimental and theoretical angular distributions, in the center-of-mass frame, for the ${}^7\text{Li} \rightarrow \alpha + t$ breakup for ${}^7\text{Li}$ incident on protons at 38.1 MeV. The experimental data, corresponding to the first kinematical solution, are denoted by filled red circles while the data corresponding to the second kinematical solution are denoted by green stars. The solid black line represents the result of the full CDCC calculation. The dot-dashed blue curve denotes the contribution of breakup via the 4.63 MeV $7/2^-$ resonance, multiplied by a factor of 20 in order to make it visible.

CDCC calculation reinforces the realism of the “philosophy” behind the CDCC approach. Comparison of gated and ungated energy spectra of the fragments in the laboratory system, the gated one being obtained by taking into account the specific geometry of MAGNEX and the silicon detector and the angular range covered, gave the efficiency of the detection system. For the transformation of the laboratory cross sections to the center-of-mass frame, for each pair of laboratory angles ($\theta_{\text{pair}} = 0.5^\circ\text{--}5^\circ, 1.0^\circ\text{--}5^\circ, 1.5^\circ\text{--}5^\circ$, etc.) the corresponding -of-mass angles for both kinematical solutions were calculated, taking into account the appropriate relations according to Ohlsen [16]. Using the CDCC calculation a mean excitation energy (weighted with the cross section of each state) for the breakup system was then attributed to each of these angles. Finally, the appropriate Jacobians were deduced for this excitation energy. The resulting angular distributions for both kinematical solutions are displayed in Fig. 5.

III. CDCC CALCULATIONS AND DISCUSSION

The CDCC calculation was performed using the code FRESKO [17]. Nuclei such as ${}^7\text{Li}$ may be modeled as two inert clusters, and the Coulomb and nuclear excitations can then be calculated from the interactions of each cluster with the target using Watanabe-type folding. The $\alpha + t$ cluster model of ${}^7\text{Li}$ was therefore adopted, with all the parameters of the model including discretization and truncation of the continuum as described in detail in Ref. [18]. The maximum excitation energy was taken as the available energy of the system above threshold, 2.283 MeV. The $\alpha + t$ continuum was divided into bins in momentum (k) space of width $\Delta k = 0.125 \text{ fm}^{-1}$, and relative angular momenta $L = 0, 1, 2, 3$ were included. The convergence of the results was tested with smaller momentum bins and angular momenta up to $L = 4$. The $7/2^-$ resonance at 4.63 MeV was treated as a continuum bin with a width of 0.2 MeV. Couplings to the first excited state at 0.478 MeV and ground state reorientation were also included. Special care was given to the optical potentials between each cluster and the target, i.e. the $p + \alpha$ and $p + t$ potentials. Empirical potentials were obtained by fitting existing $p + \alpha$ and $p + t$ elastic scattering data at the appropriate energy, $E \approx 6 \text{ MeV/u}$ [19–22]. These data were fitted with volume Woods-Saxon form factors for both real and imaginary parts for the $p + \alpha$ system and volume real and volume + surface imaginary terms for the $p + t$ system. A proton spin-orbit potential of Thomas form with parameters $V_{\text{so}} = 9.96 \text{ MeV}$, $r_{\text{so}} = 1.35 \text{ fm}$, $a_{\text{so}} = 0.69 \text{ fm}$ was added to the diagonal ${}^7\text{Li} + p$ Watanabe folding potentials. The input potentials thus obtained were fed into the FRESKO calculations and the results for ${}^7\text{Li} + p$ are compared with the elastic scattering data in Fig. 1. The full calculation (labeled “CDCC”) is in good agreement with the data. Also plotted on Fig. 1 are two curves, labeled “1 - channel” and “2 - channel,” which include couplings to the ground state reorientation only

and coupling to the 0.478 MeV first excited state of ${}^7\text{Li}$ respectively. It is thus seen that coupling to the continuum has the most important influence. Note, however, that the most important contribution is from coupling to the 4.63 MeV resonant state. This is in complete contrast to the predicted breakup cross sections for direct and resonant breakup, 65.2 and 0.55 mb respectively, supporting the previous suggestion that the influence of coupling to the continuum is not correlated with the magnitude of the breakup cross section. We also note the negligible effect of coupling to the 0.478 MeV $1/2^-$ bound state, in spite of the large cross section for populating this state, 49 mb. The calculated breakup angular distributions are compared with the data in Fig. 5. In general, the experimental results support the theory in a satisfactory way, both quantitatively and qualitatively, although theory shows a slight underestimation of the data at backward angles. It should be noted, however, that a 5% reduction in the estimated excitation energy of ${}^7\text{Li}^*$ in the simulation can produce a 20% reduction in the experimental breakup cross section. Integrating the angular distributions, we obtain for the CDCC calculation a value of $\sigma_{\text{break}} = 66 \text{ mb}$ and for the experiment a value of $\sigma_{\text{break}} = 72 \pm 15 \text{ mb}$, in excellent agreement with theory. This comprises $\sim 9\%$ of the calculated total reaction cross section, $\sigma = 722 \text{ mb}$. The good reproduction of the experimental breakup data by the CDCC calculation reinforces our conclusions concerning the breakup coupling influence. Also plotted on Fig. 5 is the angular distribution for resonant breakup via the 4.63 MeV state, multiplied by a factor of 20 in order to be visible, graphically demonstrating the negligible size of the cross section.

In summary, we have presented both experimental and theoretical results for the breakup of ${}^7\text{Li}$ incident on protons at 38.1 MeV (5.44 MeV/nucleon). The measured breakup and elastic scattering results at the same energy were well described by the same CDCC calculation. A Monte Carlo simulation of the reaction (to determine the efficiency of the detection system) based on the CDCC binning of the continuum described well the energy distributions of the breakup fragments and therefore the kinematics of the reaction, further supporting the realistic description of the breakup within the CDCC approach. A rather low breakup cross section of 66 mb was determined, attributed essentially exclusively to direct excitation to the continuum since the incident energy was such that the ${}^7\text{Li}$ 4.63 MeV $7/2^-$ resonance was barely excited. However, while the contribution to the total breakup cross section from resonant breakup was negligible, less than 1 mb, its coupling influence on the elastic scattering was found to be dominant, thus providing a striking example of an effectively virtual but nevertheless strong coupling.

ACKNOWLEDGMENT

We warmly acknowledge the TANDEM accelerator staff of LNS for the production and delivery of the ${}^7\text{Li}$ beams.

- [1] N. Keeley, N. Alamanos, K. W. Kemper, and K. Rusek, *Prog. Part. Nucl. Phys.* **63**, 396 (2009).
 [2] N. Keeley, K. W. Kemper, and K. Rusek, *Eur. Phys. J. A* **50**, 145 (2014).

- [3] L. F. Canto, P. R. S. Gomes, R. Donangelo, J. Lubian, and M. S. Hussein, *Phys. Rep.* **596**, 1 (2015).
 [4] P. R. S. Gomes, J. Lubian, L. F. Canto *et al.*, *Few Body Syst.* **57**, 165 (2016).

- [5] N. Keeley, R. S. Mackintosh, and C. Beck, *Nucl. Phys. A* **834**, 792c (2010).
- [6] A. Pakou, V. Soukeras, F. Cappuzzello *et al.*, *Phys. Rev. C* **94**, 014604 (2016).
- [7] F. Cappuzzello, C. Agodi, D. Carbone, and M. Cavallaro, *Eur. Phys. J. A* **52**, 167 (2016).
- [8] V. Soukeras, A. Pakou, F. Cappuzzello *et al.*, *Phys. Rev. C* **91**, 057601 (2015).
- [9] M. Cavallaro, F. Cappuzzello, D. Carbone *et al.*, *Eur. Phys. J. A* **48**, 59 (2012).
- [10] D. Carbone, F. Cappuzzello, and M. Cavallaro, *Eur. Phys. J. A* **48**, 60 (2012).
- [11] F. Cappuzzello, M. Cavallaro, A. Cunsolo *et al.*, *Nucl. Instrum. Methods Phys. Res., Sect. A* **621**, 419 (2010).
- [12] F. Cappuzzello, D. Carbone, and M. Cavallaro, *Nucl. Instrum. Methods Phys. Res., Sect. A* **638**, 74 (2011).
- [13] M. Cavallaro, F. Cappuzzello, D. Carbone *et al.*, *Nucl. Instrum. Methods Phys. Res., Sect. A* **648**, 46 (2011).
- [14] M. Cavallaro, F. Cappuzzello, D. Carbone *et al.*, *Nucl. Instrum. Methods Phys. Res., Sect. A* **637**, 77 (2011).
- [15] O. Sgouros, V. Soukeras, and A. Pakou, MULTIP: Multipurpose Monte Carlo simulation code for three and four body kinematics (unpublished).
- [16] G. G. Ohlsen, *Nucl. Instrum. Methods* **37**, 240 (1965).
- [17] I. J. Thompson, *Comput. Phys. Rep.* **7**, 167 (1988).
- [18] K. Rusek, P. V. Green, P. L. Kerr, and K. W. Kemper, *Phys. Rev. C* **56**, 1895 (1997).
- [19] G. Freier, E. Lampi, W. Sleator, and J. H. Williams, *Phys. Rev.* **75**, 1345 (1949).
- [20] P. D. Miller and G. C. Phillips, *Phys. Rev.* **112**, 2043 (1958).
- [21] J. E. Brolley, Jr., T. M. Putnam, L. Rosen, and L. Stewart, *Phys. Rev.* **117**, 1307 (1960).
- [22] R. Kankowsky, J. C. Fritz, K. Kilian, A. Neufert, and D. Fick, *Nucl. Phys. A* **263**, 29 (1976).